JOURNAL OF GEOPHYSICAL RESEARCH, VOL. 96, NO. B7, PAGES 11,805–11,816, JULY 10, 1991

High-Temperature Thermodynamic Properties of Forsterite

PHILIPPE GILLET

Laboratoire de Minéralogie Physique, Université de Rennes I

PASCAL RICHET AND FRANÇOIS GUYOT

Institut de Physique du Globe, Paris

GUILLAUME FIQUET

Laboratoire de Minéralogie Physique, Université de Rennes I

The high-temperature thermodynamic properties of forsterite were reviewed in the light of a new determination of the isobaric heat capacity (C_p), up to 1850 K, and Raman spectroscopic measurements, up to 1150 K and 10 GPa. The C_p measurements and available data on thermal expansion (α) and bulk modulus (K) show that the isochoric specific heat (C_v) exceeds the harmonic limit of Dulong and Petit above 1300 K. This intrinsic anharmonic behavior of C_v can be modeled by introducing anharmonic parameters $a_i = (\partial \ln \nu_i / \partial T)_V$ which are calculated from the measured pressure and temperature shifts of the vibrational frequencies. These parameters are all negative, with absolute values lower for the stretching modes of the SiO_4 tetrahedra ($a_i \approx -1 \times 10^{-5}$ K^{-1}) than for the lattice modes ($a_i \approx -2 \times 10^{-5}$ K^{-1}). Through the relation $C_p = C_v + \alpha^2 K_T V T$, the calculated anharmonic C_v and the measured C_p are then used to determine the temperature dependences of the thermal expansion and bulk modulus of forsterite, up to 2000 K, in agreement with recent experimental results. Finally, all these data point to an inconsistency for the Grüneisen parameter of forsterite, whereby the macroscopic parameter $\gamma = \alpha V K_T / C_v$ cannot be evaluated simply at high temperature by summation of the individual isothermal mode Grüneisen parameters $\gamma_{iT} = K_T (\partial \ln \nu_i / \partial P)$.

1. Introduction

A great many mantle minerals are not amenable to thermodynamic measurements because of their instability at moderate temperatures or of the minute amounts of material that can be synthesized. To setup thermodynamic models of mantle phase equilibria, use is thus made of spectroscopically determined heat capacities and entropies [e.g., *Kieffer*, 1979]. The difficulty with this approach, however, is that there are virtually no measurements for testing the validity of the method under the high-temperature conditions of the mantle.

Forsterite is probably the mineral that has been studied the most extensively. The purpose of this contribution is thus to consider forsterite as a model mineral to investigate the consistency of the thermodynamic and spectroscopic data from ambient up to high pressures and temperatures. Our purpose is not to model mineral properties in the most comprehensive way, as done for example in the lattice dynamics study of forsterite by *Rao et al.* [1988], and the reasons for our simplified approach are twofold. First, experiments like inelastic neutron scattering are not feasible on minerals for which thermodynamic measurements are lacking. Thus we will consider only spectroscopic data that can be gathered on high-pressure phases. Second, lattice-dynamics calculations are still done within the framework of the quasi-harmonic approximation whose limitations at high temperatures must be assessed. As a matter of fact, the role of anharmonicity can be investigated rather simply from the limited spectroscopic information that can be obtained for mantle minerals [*Gillet et al.*, 1989].

In this paper we are mainly interested in the isobaric(C_p) and isochoric (C_v) heat capacities, thermal expansion coefficient (α) and isothermal bulk modulus (K_T) of forsterite. Through calculations of the heat capacity from spectroscopic data, we first show that anharmonicity contributes significantly to C_v and the other thermodynamic properties of forsterite above 1300 K. Then we discuss the consistency of the available C_p, α and K_T data at high temperature. Finally, we discuss the Grüneisen parameter of forsterite, in both macroscopic and microscopic terms. To complement the available experimental data base needed for our purpose, we have also redetermined the heat capacity of forsterite between 800 and 1800 K and measured the pressure and temperature dependences of the Raman-active vibrational frequencies of forsterite.

2. Experimental Methods

Calorimetric measurements were made with the ice calorimeter, high-temperature equipment and experimental procedures described by *Richet et al.* [1982], with the slight modifications reported by *Richet and Bottinga* [1984]. About 5-6 g of forsterite, contributing from 60 to 65% to the total measured heat content, were run in a Pt-Rh 15% crucible.

Paper number 91JB00680
0148-0227/91/91JB-00680$05.00

Measurements under the same conditions on α-Al_2O_3, the calorimetric standard, suggest instrumental inaccuracies of about 0.2 and 0.5% for the relative enthalpies and heat capacities, respectively [*Richet et al.*, 1982].

The forsterite specimen used for calorimetric measurements, of industrial origin, was given by O. Jaoul (Université Paris XI). Its composition, as determined from electron-microprobe analyses with the automated CAMEBAX microprobe of the Université Paris VI is 0.11 (2) wt % Al_2O_3, 42.61 (3) wt % SiO_2, 57.36 (4) wt % MgO and 0.05 (2) wt % CaO, total of 100.15 (6). This compares favorably with the nominal composition, namely 42.70 and 57.30 wt % SiO_2 and MgO, respectively. The lattice parameters a = 4.760 (1), b = 10.201 (2) and c = 5.985 (1) Å were derived from an Xray powder diffraction pattern in which the reflections of only forsterite were apparent. Hence, the molar mass used was the nominal one. Spectroscopic measurements were performed on a synthetic specimen of similar quality.

The Raman spectra were recorded with the multichannel microprobe (Microdil 28, from Dilor) of the MLRO service of the University of Nantes. The light was collected in the backscattering direction through a Leitz UTK 40 or UTK 50 objective (focal distance of 8 or 18 mm; numerical aperture of 0.63 or 0.32, respectively). The spectra were obtained from about 10 accumulations lasting each 20 to 40 s, and peak positions were identified to within ± 1 cm^{-1}. To record a maximum number of bands at high temperatures, small single crystals were inserted with different orientations into the heating stage of a microscope. Temperatures were measured within a few degrees with a Pt-PtRh 10 % thermocouple. A diamond-anvil cell was used to compress the sample in the 200-μm hole of a stainless-steel gasket to record the high-pressure spectra. A 4:1 ethanol-methanol mix was used as a pressure-transmitting medium for all experiments, and pressures were measured with the ruby-fluorescence method.

3. CALORIMETRY

In spite of the considerable geophysical importance of forsterite, calorimetric measurements have long been scarce and the relative enthalpies of *Orr* [1953] up to 1800 K were the only available high-temperature data. Our experimental relative enthalpies (Table 1) are about 1 % lower than the results of Orr, except at the highest temperatures where the difference tends to decrease. This is apparent in Figure 1 where both data sets are plotted in the form of mean heat capacities, $C_m = (H_T - H_{273})/(T-273)$.

TABLE 1. Relative Enthalpy of Forsterite (kJ/mol)

Run	T, K	$H_T - H_{273}$
BD.8	787.9	75.718
BD.3	922.3	99.519
BD.11	977.0	109.12
BD.9	1087.0	128.41
BD.4	1123.3	135.64
BD.2	1264.2	160.30
BD.5	1374.2	180.44
BD.1	1615.6	225.85
BD.7	1493.8	202.44
BD.10	1722.1	246.15
BD.12	1847.1	270.75

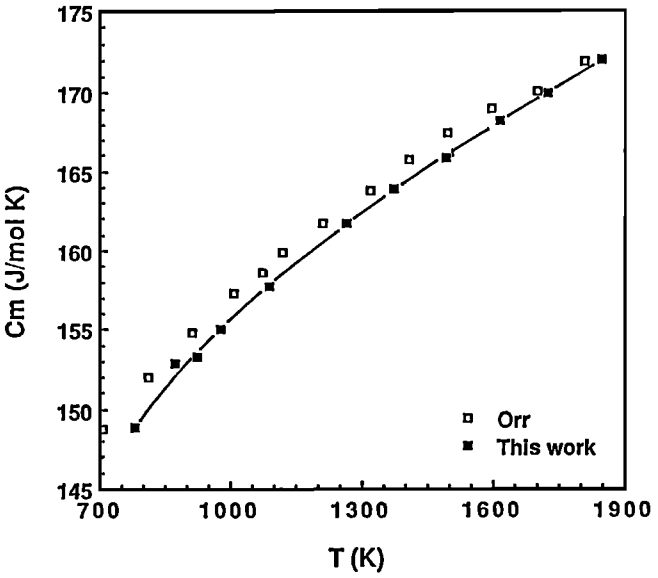

Fig. 1. Mean heat capacity of forsterite. Open squares: results of *Orr* [1953], referred to 273 K with the $H_{298} - H_{273}$ of *Robie et al.* [1982]; solid squares: this work.

A simultaneous least-squares fit was made to the experimental C_p and enthalpy data to obtain the following equations of the form recommended by *Haas and Fisher* [1976], *Berman and Brown* [1985] and *Richet and Fiquet* [1991], respectively:

$$C_p = 297.570 - 55.684\ 10^{-3}\ T - 5.187\ 10^5/T^2 - 2731.7\ T^{0.5} + 19.791\ 10^{-6}\ T^3, \quad (1)$$

$$C_p = 241.777 + 2119.3/T^{0.5} + 1.5657\ 10^6/T^2 - 4.7258\ 10^8/T^3, \quad (2)$$

$$C_p = -402.753 + 74.290\ \ln T + 87.588\ 10^3/T - 25.913\ 10^6/T^2 + 25.374\ 10^8/T^3, \quad (3)$$

At low temperatures, the adiabatic C_p of *Kelley* [1943], down to 50 K only, have been superseded by those of *Robie et al.* [1982] for the wider temperature interval 5-380 K. Our results join smoothly with both sets of measurements which are in mutual agreement, as indicated by the deviations of the values given by equations (1)-(3) from the experimental data (Table 2). These results also agree, to within their greater error margins, with the Differential Scanning Calorimetry (DSC) measurements of *Watanabe* [1982] and *Ashida et al.* [1987].

The heat capacities reported in these different studies are plotted in Figure 2. Up to 1600 K, the consistency of all the data is to within ± 1 % in the temperature range of the various measurements. Above 1600 K, the anomalously high heat capacities given by the equation reported by *Orr* [1953] and (1) result from the analytical forms of these equations that do not allow high-temperature extrapolations. As discussed by *Richet and Fiquet* [1991], equation (3) is to be preferred for this purpose whereas (2) gives apparently too low values because, in contrast to (1) and (3), it does not reproduce the

TABLE 2. Average Absolute Deviations (AAD) of Values Given by Equations (1), (2) and (3) From The Experimental C_p and Enthalpy Data

Reference	Property	N	ΔT, K	AAD, % (1)	(2)	(3)
Kelley [1943]	C_p	3	276-295	0.31	0.39	0.23
Robie et al. [1982]	C_p	22	270-380	0.08	0.18	0.06
Watanabe [1982]	C_p	8	350-700	0.43	0.63	0.33
Ashida et al. [1987]	C_p	10	280-700	1.10	0.75	0.84
Orr [1953]	H	16	398-1808	0.82	0.75	1.15
This Work	H	11	782-1847	0.05	0.15	0.06

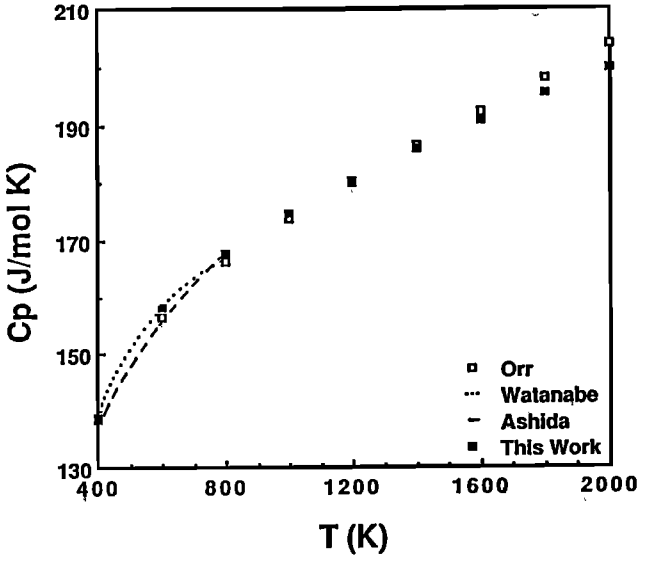

Fig. 2. Heat capacity of forsterite as reported by *Orr* [1953], *Robie et al.* [1982], *Watanabe* [1982], *Ashida et al.* [1987], and in this work.

experimental data to within their error margins. This is apparent in Table 2 for the measurements of *Robie et al.* [1982] and ours. In the following sections, the heat capacity will thus be obtained from (3), with an uncertainty that is estimated to be lower than 1 % up to 2000 K at least.

4. Spectroscopy

As shown below, accurate calculations of the heat capacity require comprehensive high-pressure and high-temperature spectroscopic data. Previous Raman and infrared measurements on forsterite have been reviewed by *Hofmeister* [1987] and *McMillan and Hofmeister* [1988]. Briefly, the high vibrational frequencies, between 800 and 1000 cm^{-1}, have been assigned to combinations of symmetric and asymmetric stretching modes of the SiO_4 tetrahedra. A gap in the range 800 - 650 cm^{-1} separates these modes from the lower-frequency part of the spectrum, which includes the bending modes of the SiO_4 tetrahedra and the lattice modes involving the MgO_6 octahedra.

To fill in the lack of high-temperature measurements, we have recorded the Raman spectrum of forsterite up to 1150 K at ambient pressure. The usual band broadening at high-temperatures is apparent in Figure 3 and the negative variations with temperature of the frequencies are linear within experimental uncertainties (Table 3 and Figure 4). The relative frequency shifts plotted in Figure 5 as a function of wavenumber show that the internal modes depend less on temperature than the lattice modes. This is also apparent in Table 3 which lists the corresponding isobaric Grüneisen parameters:

$$\gamma_{iP} = -1/\alpha\,(\partial \ln \nu_i/\partial T)_P \qquad (4a)$$

which were calculated with the 1-bar, 298 K thermal expansion coefficient.

At room temperature, infrared measurements up to 42.5 GPa have been reported by *Hofmeister et al.* [1989], and the available Raman data [*Besson et al.*, 1982; *Gillet et al.*, 1988; *Chopelas*, 1990] extend up to 22.7 GPa. For intercomparison purposes and for estimating better the uncertainties on the shifts, we have also recorded the room-temperature Raman spectrum of forsterite up to 5.5 GPa. Measurements were made with both increasing and decreasing pressures or temperatures. No hysteresis was observed. Typical examples of the spectra at pressure are given in Figure 6. Qualitatively, the two frequency ranges found under ambient conditions are still observed at pressure, with only linear increases of the vibrational frequencies with pressure (Table 3).

Above 10 GPa, *Chopelas* [1990] and *Hofmeister et al.* [1989] have interpreted minor changes in the vibrational pattern in terms of a phase transition and we will thus restrict ourselves to pressures lower than 10 GPa where our high-pressure results agree with the more extensive data of *Chopelas* [1990], see Table 3 and Figure 7. The relative changes in frequency of the internal modes of the SiO_4 tetrahedra depend clearly less on pressure than those of the lattice modes, as previously pointed out by *Hofmeister et al.* [1989] and *Chopelas* [1990]. This is also shown in Table 3 by the corresponding isothermal Grüneisen parameters:

$$\gamma_{iT} = K_T\,(\partial \ln \nu_i/\partial P)_T \qquad (4b)$$

which were calculated with the 1-bar, 298 K bulk modulus.

5. Anharmonicity and Heat Capacity

Macroscopic Evidence

The isochoric heat capacity (C_V) is related to the measurable isobaric heat capacity by:

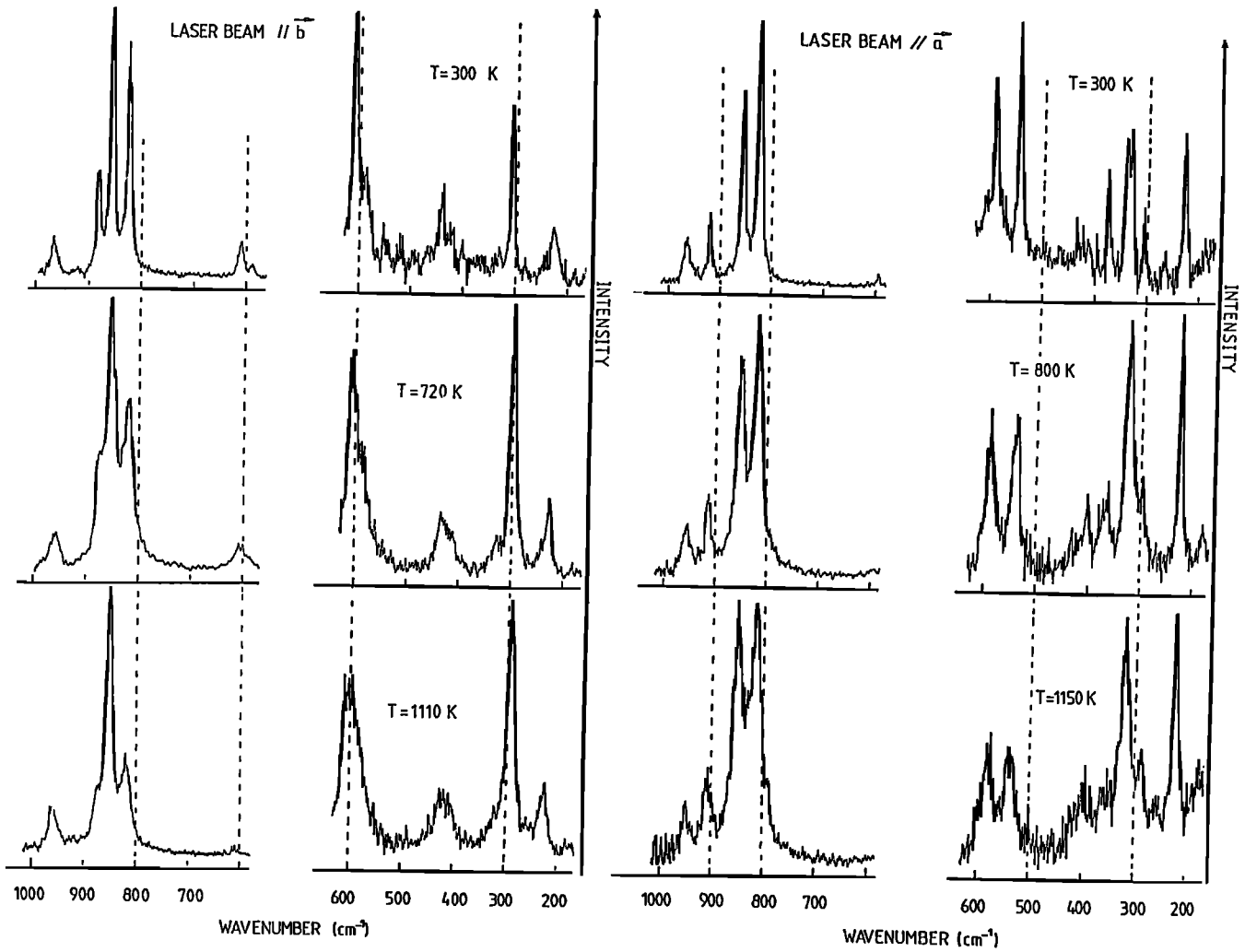

Fig. 3. Raman spectrum of forsterite at three temperatures with the laser beam parallel to either the *a* or the *b* axis. The intensity differences result from polarization effects inherent to the collecting geometry of the microRaman setup.

$$C_V = C_p - TV\alpha^2 K_T. \quad (5)$$

Departure of C_V from the limit of Dulong and Petit, namely 3R/g atom (R = gas constant) is a traditional measure of intrinsic anharmonicity. In Figure 8 we have plotted C_V as calculated from equations (5) and (3) and the most recent high-temperature measurements of α and K_T by *Kajiyoshi* [1986] and *Isaak et al.* [1989]. The Dulong-and-Petit limit is passed at about 1300 K and the excess C_V over this limit reaches about 5 % at 2000 K. In other words, the $TV\alpha^2K_T$ term of C_p accounts for only part of the vibrational anharmonicity. As stated previously by *Anderson and Suzuki* [1983] from older data, forsterite thus clearly displays intrinsic anharmonicity at high temperature, a conclusion also reached when one uses other values of α such as those plotted in Figure 2 of *Isaak et al.* [1989]. Such an effect is not apparent in simple compounds like MgO and CaO for which the Dulong and Petit limit for C_V is not exceeded at high temperature [*Anderson and Zou*, 1990]. An explanation is that in these oxydes the phonons are only weakly coupled whereas, in complex structures like forsterite, strong coupling (and thus intrinsic anharmonicity) is expected.

Anharmonic Calculation of the Heat Capacity

Heat capacity calculations are usually made within the harmonic approximation, i.e., with the assumption that vibrational frequencies are independent of temperature. Regardless of the details of this kind of analysis, the main point is that the contribution of each acoustic or optic mode to the heat capacity is in fact that of an harmonic, Einstein oscillator:

$$C_{Vi}^{h} = k\,(h\nu_i/kT)^2 \exp(h\nu_i/kT)\,/[\exp(h\nu_i/kT) - 1]^2 \quad (6)$$

where the frequency ν_i is independent of temperature, and h and k are the Planck and Boltzmann constants.

As shown in Figure 4 for forsterite, one observes that vibrational frequencies do vary with temperature. In the quasi-harmonic approximation, these variations are simply accounted for by allowing the frequencies to be temperature dependent in equation (6). Thus, in both the harmonic and quasi-harmonic approximations, the high-temperature limit of C_V is $3R/g$ atom since the high-temperature limit of an Einstein oscillator is k. In other words, it is assumed that the anharmonic contribution to C_V is negligible, and that

TABLE 3. Pressure and Temperature Shifts of Vibrational Frequencies, and Anharmonic Parameters

ν_i, cm^{-1}	γ_{iT}*	γ_{iT}†	γ_{iT}≠	$(\partial\nu_i/\partial T)$†, cm^{-1}/K	γ_{iP}†	a_i†, 10^{-5} K^{-1}
967	0.66	0.7		-0.027 (2)	1.07 (16)	-1.07(32)
920	0.38	0.4	0.54	-0.019 (2)	0.82 (14)	-1.16(35)
882	0.44	0.5	0.49	-0.023 (2)	1.00 (16)	-1.46(44)
856	0.49	0.5		-0.016 (1)	0.72 (10)	-0.60(18)
825	0.48	0.5	0.54	-0.017 (1)	0.79 (10)	-0.81(20)
610	0.70	0.7		-0.013 (1)	0.82 (15)	-0.31 (9)
593				-0.012 (1)	0.85 (13)	
585	0.66	0.6		-0.013 (1)	0.85 (13)	-0.51(15)
548	0.53	0.6		-0.011 (1)	0.77 (13)	-0.63(19)
443	1.60	1.8		-0.029 (2)	2.52 (36)	-2.38(71)
426	1.41			-0.018 (2)	1.62 (30)	-0.58(17)
414	0.99			-0.022 (2)	2.04 (30)	-2.74(82)
376	1.25	1.4		-0.019 (2)	1.94 (35)	-1.79(54)
341	1.87			-0.025 (2)	2.82 (43)	-2.51(75)
334	1.16	1.3		-0.019 (2)	2.18 (39)	-0.81(24)
307	1.63	1.8		-0.023 (2)	2.87 (46)	-3.22(96)
244	1.21			-0.018 (1)	2.13 (27)	-3.10(93)
232	0.67	0.7		-0.011 (1)	1.82 (27)	-3.00(90)
183	2.09			-0.012 (1)	2.51 (37)	-1.12(34)
171§	1.47			-0.012 (2)	2.60 (62)	-3.0 (15)
99§	1.04			-0.008 (2)	2.99 (97)	-5.0 (25)

* Data from *Chopelas* [1990]

† Results from the present study. Uncertainties for a_i obtained from $\alpha = 2.7 \pm 0.2$ x10^{-5} K^{-1}, a 15 % uncertainty on γ_{iT} and the reported uncertainties on the γ_{iP}

≠ Data from *Besson et al.* [1982]

§ Acoustic modes: γ_{iT} from *Chopelas* [1990] and γ_{iP} calculated from the acoustic data of *Isaak et al.* [1989].

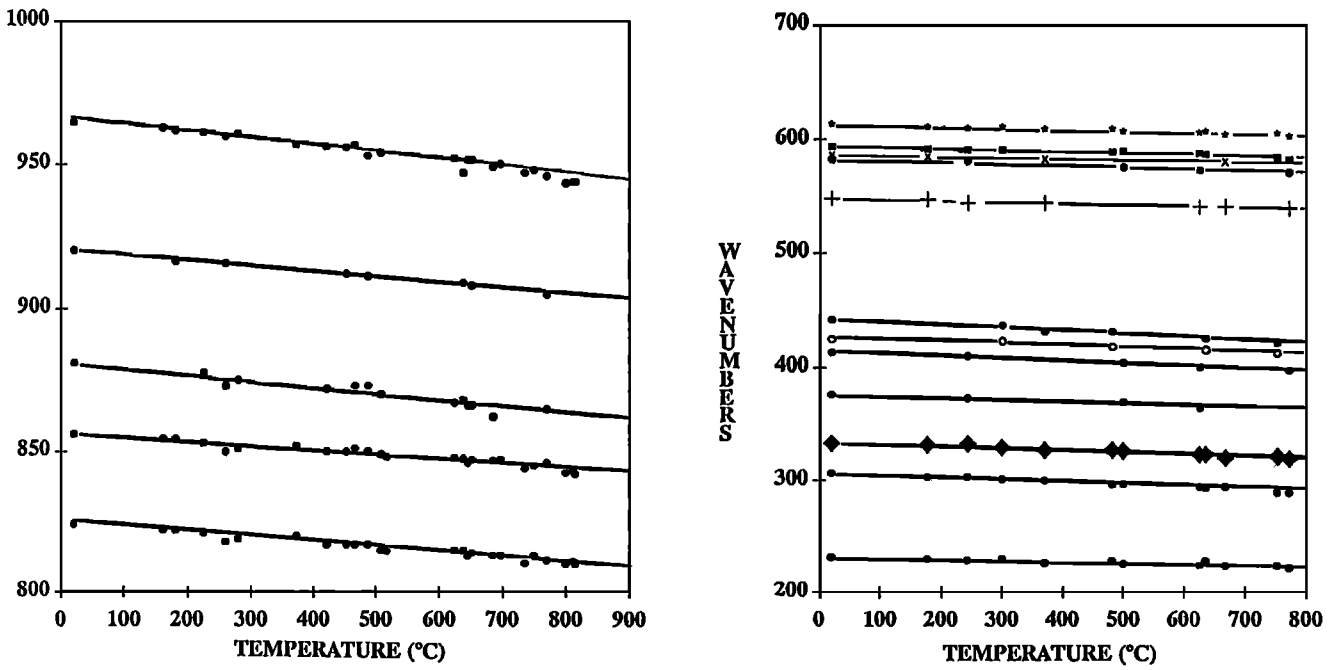

Fig. 4. Temperature dependence of the vibrational frequencies. The symbol size is similar to the errors of the data.

anharmonicity (often called extrinsic anharmonicity) contributes to C_p in (5) through the thermal expansion coefficient α only.

For forsterite, Kieffer modeling [*Hofmeister*, 1987; *Chopelas*; 1990] or lattice dynamical calculations [*Price et al.*, 1987; *Rao et al.*, 1988; *Choudury et al.*, 1989] have been performed up to 1000 K with either the harmonic or quasi-harmonic assumptions. In view of the excess C_v over the Dulong-and-Petit limit shown by forsterite, a calculation of the intrinsic anharmonic contribution to C_v itself must be

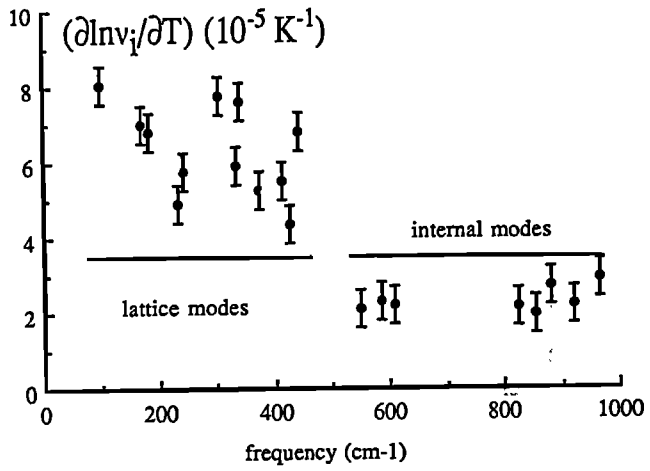

Fig. 5. Relative changes in internal and lattice vibrational frequencies with temperature. The absolute values are represented, but all the shifts are in fact negative.

performed. *Gillet et al.* [1989] pointed out that this contribution can be determined simply from high-pressure and high-temperature spectroscopic measurements. To demonstrate this result in a more rigorous way, we will characterize the intrinsic anharmonicity of a vibrational mode i by the variation of ν_i with temperature at constant volume. We will use for this purpose the anharmonic parameters a_i introduced by *Mammone and Sharma* [1979]:

$$a_i = (\partial \ln \nu_i / \partial T)_V = \alpha K_T (\partial \ln \nu_i / \partial P)_T + (\partial \ln \nu_i / \partial T)_P. \quad (7)$$

The parameter a_i can also be expressed as

$$a_i = \alpha (\gamma_i T - \gamma_i P) \quad (8)$$

and thus it can be determined from the pressure and temperature dependences of ν_i through (4*a*)-(4*b*). These parameters at 298 K and 1 bar are listed in Table 3 for forsterite, along with their uncertainties as obtained from the spectroscopic results. Note in Figure 9 that the absolute values of these parameters are lower for the internal modes of SiO_4 tetrahedra than for the lattice modes.

As we will show now, the usefulness of the a_i parameters is that the isochoric heat capacity of an ensemble of anharmonic oscillators is simply related to the harmonic heat capacities:

$$C_V = \Sigma C_{Vi}^h (1 - 2a_i T) = C_V^h - T \Sigma 2a_i C_{Vi}^h \quad (9)$$

where C_V^h, the harmonic part of the heat capacity, can be obtained with a suitable model in which the room-temperature and pressure frequencies are used. To demonstrate equation (9), we begin with the internal energy of the ensemble of oscillators which is related to the partition functions of the individual oscillators (Z_i) by:

$$U = U_0 + \Sigma kT^2 (\partial \ln Z_i / \partial T)_V \quad (10)$$

where U_0 is the lattice cohesive energy. For an harmonic oscillator, the partition function is:

$$Z_i = \exp(-h\nu_i/2kT)/[1 - \exp(-h\nu_i/kT)] \quad (11)$$

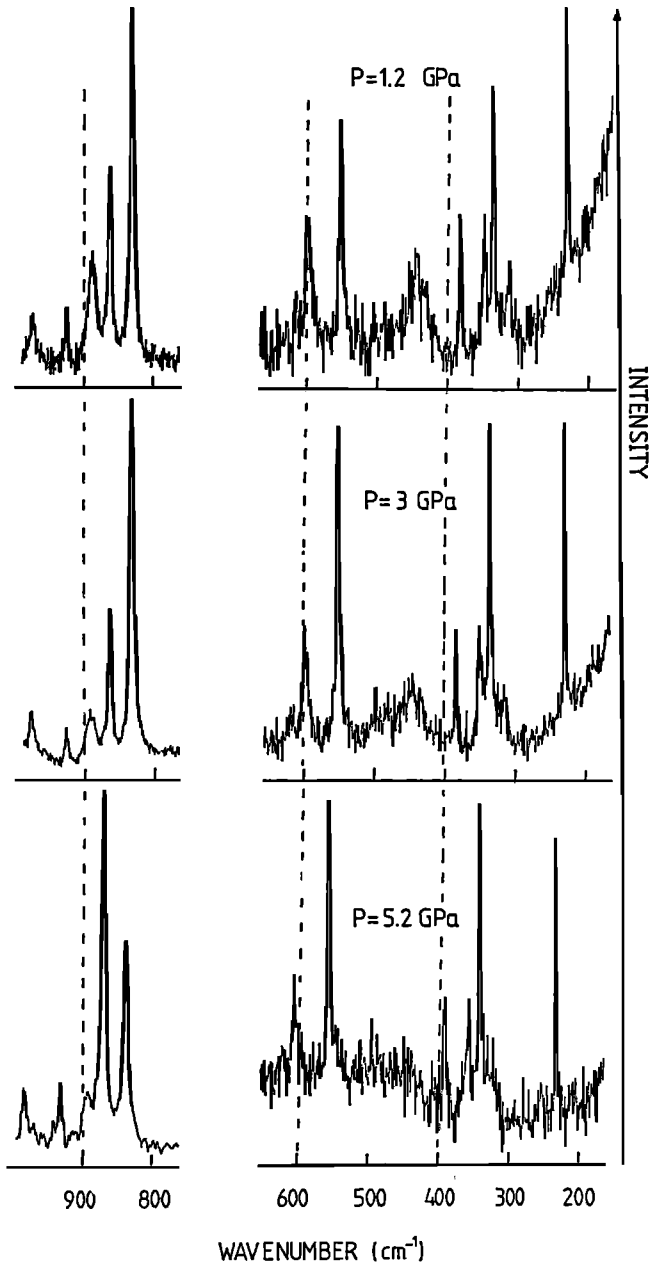

Fig. 6. Raman spectrum of forsterite at three pressures.

Spectroscopic measurements show that $(\partial \ln \nu_i / \partial T)_V$ generally differ from zero. Thus we will use (11) but we take into account the variations of the frequencies with temperature at constant volume when inserting (11) in (10) to obtain:

$$U = U_0 + \Sigma U_i^h (1 - a_i T) \quad (12)$$

where the harmonic vibrational internal energy is

$$U_i^h = h\nu_i \{1/2 - 1/[1 - \exp(h\nu_i/kT)]\} \quad (13)$$

The anharmonic C_V is thus

$$C_V = (\partial U/\partial T)_V = \Sigma \{C_{Vi}^h (1 - a_i T)^2 - T U_i^h [a_i^2 + (\partial a_i/\partial T)_V]\} \quad (14)$$

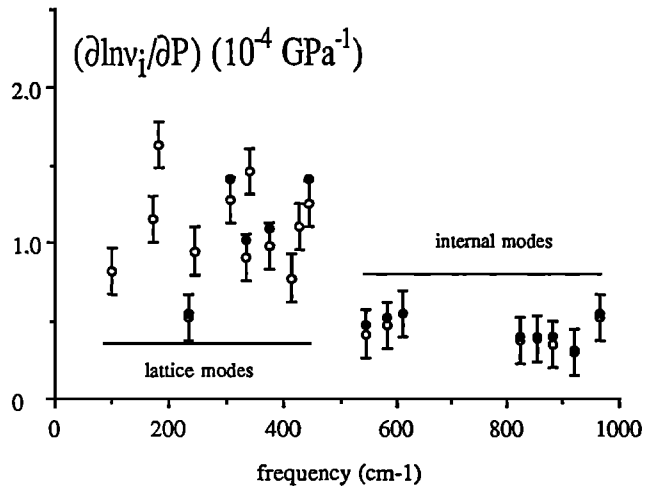

Fig. 7. Relative changes in internal and lattice vibrational frequencies with pressure. Open circles: *Chopelas* [1990]; solid circles: this work.

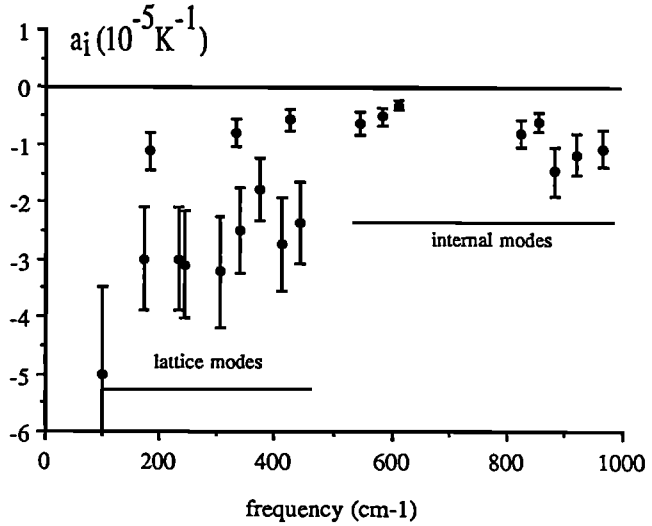

Fig. 9. Anharmonic parameters of the Raman modes of forsterite calculated at 298 K and 1 bar.

In the next section, we evaluate the various terms of (14) to show that this expression reduces numerically to the much simpler equation (9). *Gillet et al.* [1989] obtained previously for C_V:

$$C_V = \Sigma C_{Vi}^h - \Sigma a_i U_i^h - T \Sigma a_i C_{Vi}^h. \quad (15)$$

Equation (14) is more rigorous than (15) because it incorporates the contribution of the zero-point energy and takes consistently into account the variation with temperature of the vibrational frequencies. Numerically, however, (15) also reduces to (9) because U_i^h do not differ much from TC_{Vi}^h at high temperatures. For practical purposes, (9), (14) and (15) thus give nearly the same results.

Numerical Calculations

From the spectroscopic data, one finds that all the a_i parameters are of the order of -10^{-5} K^{-1} (cf. Table 3). Hence, the first term of the right-hand side of (14) can be safely reduced to (9) up to a few thousand degrees. To show that the second term is negligible, we note that the term $T U_i^h$ is about $T^2 C_{Vi}^h$ at high temperatures. Finally, $(\partial a_i/\partial T)_V$ can be determined from

$$(\partial a_i/\partial T)_V = (\partial a_i/\partial T)_P + \alpha K_T (\partial a_i/\partial P)_T. \quad (16)$$

From our results which show linear variations of the frequencies with pressure and temperature, we estimate that the two derivatives of the RHS of (16) are smaller than 10^{-9} K^{-1}. This makes it these terms negligible in (16). In summary, the parameters a_i must be considered as temperature independent in (9), a conclusion similar to that obtained by *Gillet et al.* [1990] for quartz from detailed numerical calculations of the a_i parameters.

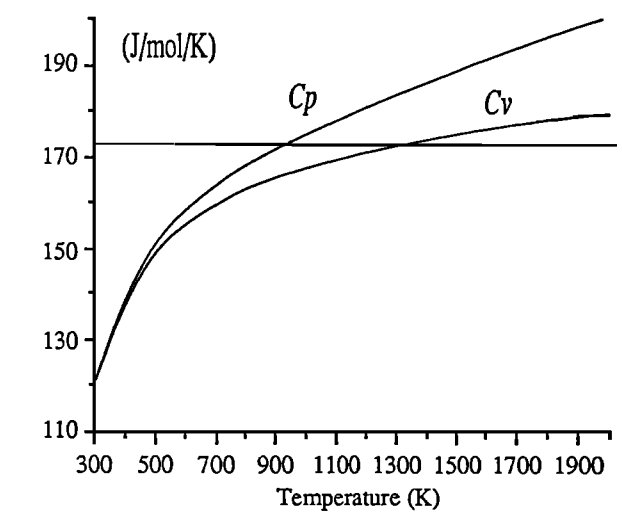

Fig. 8. Isobaric and isochoric heat capacity of forserite: C_p: given by equation (3), and C_V calculated from relation (5) with α and K_T as given by *Isaak et al.* [1989].

Application to Forsterite

All optic vibrational modes are not Raman or infrared active. For practical applications, it is thus necessary to use an averaging scheme for the observed frequencies. In Kieffer's model the contribution to C_V of a set of m optic continua is given by

$$C_V = 3nR \sum_{i=1}^{m} \frac{n_i}{N} \int_{\nu_{li}}^{\nu_{ui}} \frac{x^2 \exp(x)\, dx}{(\nu_{ui} - \nu_{li})\,[\exp(x) - 1^2]}$$

$$= 3nR \sum_{i=1}^{m} C_{Vi}^h, \quad (17)$$

with $x = h\nu_i/kT$, n is the number of atoms in the mineral formula, R is the gas constant, n_i is the number of modes in the ith continuum, N is the total number of vibrational modes, and ν_{li} and ν_{ui} are the lower and upper cutoff frequencies of the i^{th}continuum, respectively.

Using *Kieffer's* [1979] model with several optic continua, *Hofmeister* [1987] has proposed different approximations for the density of states of the optical modes of forsterite. Two of these models are shown in Figure 10, along with a third one which we have set up to account for the three different ranges of

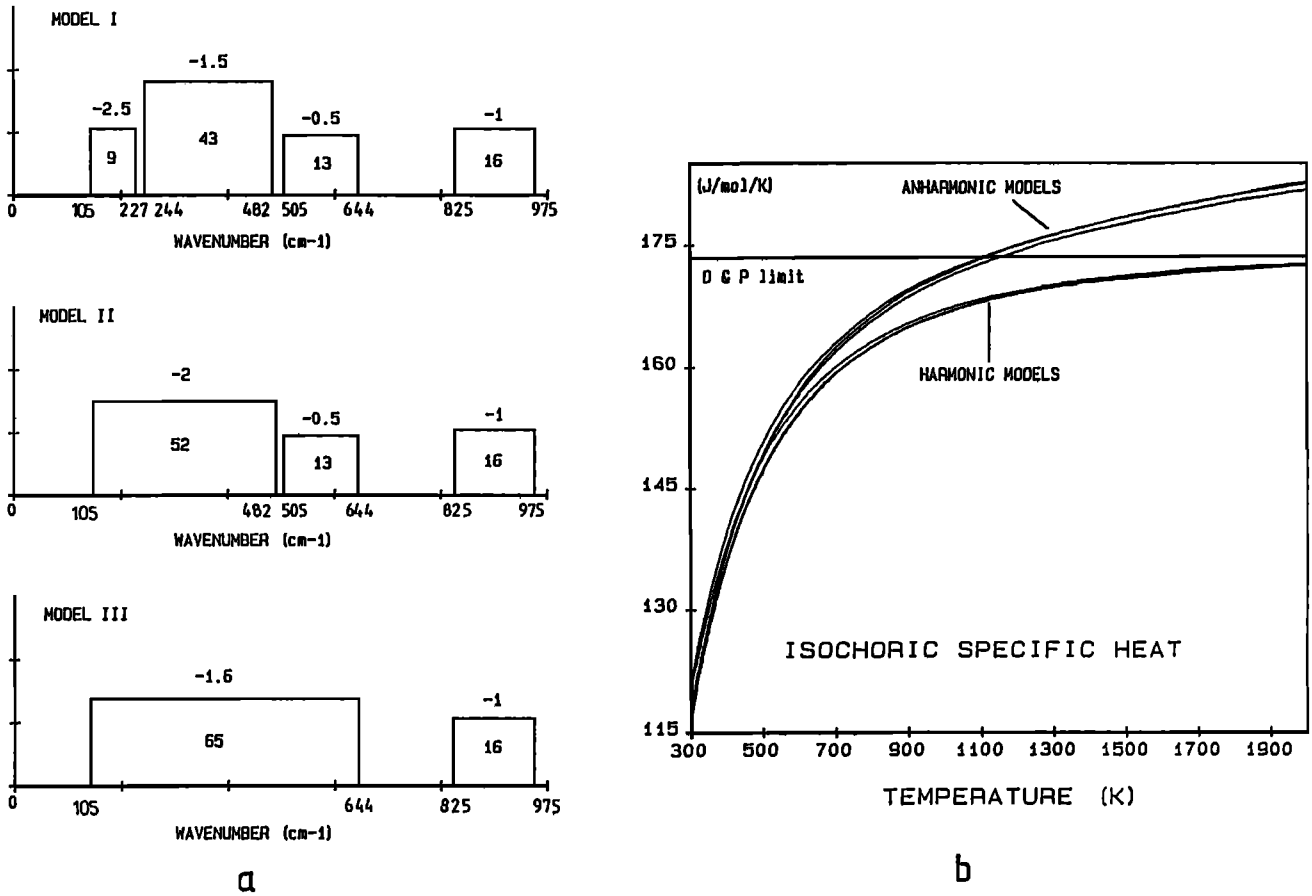

Fig. 10. (*a*) Models of density of states consistent with the spectroscopic data (acoustic modes not shown). Models I and III are adapted from *Hofmeister* [1987]. The lowest mode at 105 cm^{-1} is taken from the inelastic neutron scattering data of *Rao et al.* [1988]. The numbers in the boxes represent the number of modes in that continuum. The numbers above the boxes refer to the mean a_i parameter for those modes. (*b*) Harmonic and anharmonic C_v calculated with the densities of states shown in (a).

frequencies apparent in Figures 5 and 7. The numerical data relevant to heat capacity calculations with these three models are included in Figure 10. The remaining data, namely the acoustic velocities and molar volumes, were taken from *Kieffer* [1979] and *Hofmeister* [1987]. As usual, the results are sensitive functions of the cutoff frequencies at low temperatures, but the main result is that all models yield harmonic heat capacities differing by less than 2 and 0.5 % at 300 and 1000 K, respectively (Figure 10 and Table 4).

With the anharmonic contribution, the isochoric heat capacity is

$$C_v = 3nR \sum_{i=1}^{m} C_{vi}{}^h (1 - 2 a_i T). \qquad (18)$$

For evaluating (18) an averaging scheme must also be used for the a_i parameters. To ensure consistency with the calculation of the harmonic contribution to C_v, the a_i were averaged over the same frequency continua as used in the various Kieffer models. Calculations show that the anharmonic contribution becomes significant at about 1300 K (Figure 10 and Table 4) and reaches about 7 % at 2000 K, with values that are insensitive to the averaging scheme, and brings the calculated C_v to within 1% with the values obtained from measurements with equation (5).

6. Consistency of Thermodynamic Data

The data plotted in Figure 11 illustrate the aforementioned uncertainties on the thermal expansion coefficient of forsterite. Published values differ by 30 % between 300 and 1400 K and the differences reach 50 % when extrapolating these results up to 2000 K. To improve thermodynamic modeling, *Fei and Saxena* [1987a] and *Saxena* [1988, 1989] pointed out that equation (5) provides a simple means of ensuring consistency between thermal and volume properties. For MgO, for example, *Saxena* [1989] used experimental C_p values to optimize simultaneously α, K_T and C_v. (In passing, we note that satisfactory results could be obtained only when C_v was allowed to differ from the Dulong-and-Petit limit, i.e., when significant anharmonicity was assumed.)

Basically, we will follow the same approach, with the main difference that we greatly reduce the number of adjustable parameters by considering C_v as a known quantity obtained from anharmonic vibrational modeling. The optimization method followed has been described in detail by *Tarantola and Valette* [1982] and *Sotin* [1986]. The starting parameters are listed in Table 5, along with all the estimated uncertainties which are the greatest for the thermal expansion coefficient. Various analytical expressions have been used for α and K_T. The results depend little on the form of these equations and the following simple expressions have been found satisfactory:

TABLE 4. Isobaric and isochoric heat capacity of forsterite (J/mol K).

T(K)	C_p	C_v	calculated C_v with models≠					
	exp*	exp†	1 h	1 anh	2 h	2 anh	3 h	3 anh
300	119.2	117.9	116.8	117.7	120.1	121.1	116.7	117.5
600	158.2	154.7	154.4	156.9	155.4	158.2	154.2	156.9
900	171.4	165.6	164.9	168.9	165.3	169.8	164.8	169.1
1200	180.4	170.6	168.9	172.8	169.2	175.4	168.9	174.7
1500	188.2	175.0	170.9	178.4	171.1	178.4	170.9	177.6
1800	195.7	178.4	172.1	180.8	172.1	181.5	172.1	180.9
2000	199.6	180.0	172.3	181.2	172.3	182.1	172.3	181.6

* Values obtained with equation (3).
† Calculated from equations (3) and (5), the bulk moduli of *Isaak et al.* [1989] and the thermal expansion of *Kajiyoshi* [1986].
≠ Calculated from harmonic (h) or anharmonic (anh) vibrational modeling. The numbers refer to the various densities of states of Figure 10.

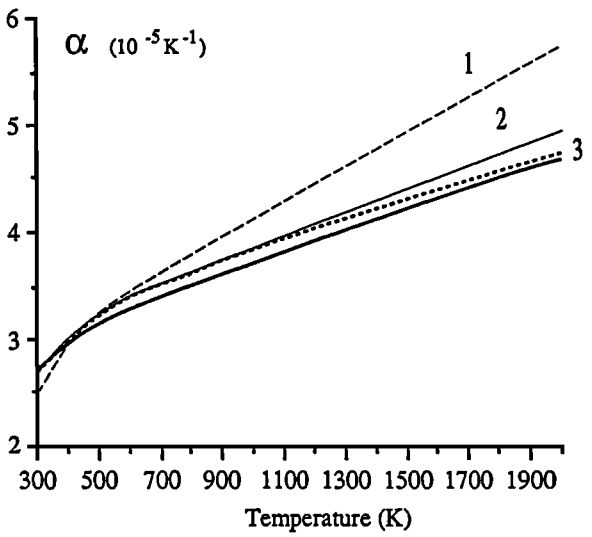

Fig. 11. Thermal expansion coefficient of forsterite. Curve 1 (dashed line) from *Suzuki et al.* [1983]; Curve 2 (thin line) from *Kajiyoshi* [1986]; curve 3 (dotted line) from *Fei and Saxena* [1987*b*]; Thick curve obtained in this work from data inversion with (5).

$$\alpha = \alpha_0 + \alpha_1 T + \alpha_2/T^2 \quad (19)$$

$$K_T = K_{T0} + (dK_T/dT)_0\, T. \quad (20)$$

Finally, the slight temperature dependence of the volume, which plays only a minor role in (5), was accounted for by

$$V = V_0 (1 + \int \alpha\, dT). \quad (21)$$

In summary, numerical values of C_p taken at 50 K intervals as given by equation (3) were used in (5), along with the anharmonic C_v calculated with the model #3 of Figure 10, to adjust the coefficients of (19) and (20).

The slight curvature with temperature of the adiabatic bulk modulus (K_S) observed by *Isaak et al.* [1989] cannot be translated to the isothermal K_T in view of the stated uncertainties of the other data appearing in equation (5).

TABLE 5. Thermal Expansion and Bulk Modulus of Forsterite up to 2000 K From Data Inversion

	Input Data* (1% Uncertainty)		Inverted Values and Uncertainties	
T,K	C_p	C_v	C_p	C_v
300	119.2	117.8	117.9	116.7
600	158.2	156.9	158.7	155.4
900	171.4	168.8	172.7	167.2
1200	180.4	172.8	181.3	172.8
1500	188.2	177.6	188.6	176.8
1800	195.2	180.8	196.2	179.2
2000	199.6	181.2	201.7	182.1

Parameters†	Apriori Values and Uncertainties	Aposteriori Values and Uncertainties
$10^5\alpha_0$	3 (2)	2.77 (9)
$10^8\alpha_1$	1 (2)	0.97 (9)
α_2	1 (10)	-0.32 (54)
K_T (kbar)	1290 (20)	1277 (20)
(dK_T/dT) (kbar/K)	-0.23 (20)	-0.20 (2)
V_o (cm^3/mol)	43.67 (30)	43.55 (41)

* Input data for C_p as given by equation (3), and C_v (anharmonic vibrational model 3 of Figure 10) taken every 50 K from 300 to 2000 K.
† Initial estimates of α, K_T, and (dK_T/dT) taken from *Fei and Saxena* [1987*b*] and *Isaak et al.* [1989], respectively.

Comparison of the derived α (Table 5) with available data in Figure 11 shows very good agreement with the high-temperature observations and extrapolations of *Kajiyoshi* [1986]. The inverted values of K_{T0} and $(dK_T/dT)_0$ listed in Table 5 are also in excellent agreement with those of *Isaak et al.* [1989].

Finally, the consistency of our derived data can be checked independently by calculating K_T from the measured K_S of *Isaak et al.* [1989], our measured C_p, and our calculated anharmonic C_v with:

$$K_T = K_S C_v/C_p. \quad (22)$$

The moduli obtained in this way are compared in Table 6 and

TABLE 6. Bulk modulus of forsterite (GPa)

T, K	K_S*	K_T†	K_T≠	K_T§
300	128.7	127.1	127.7	127.4
600	123.8	122.7	121.7	120.9
900	118.4	116.8	115.7	114.1
1200	113.0	109.4	109.7	107.0
1500	107.6	101.5	103.7	100.0
1800	101.9	94.2	97.7	93.1
2000	98.2	89.3	91.7	88.3

* Adiabatic data from *Isaak et al.* [1989].
† Calculated from $K_T = K_S C_V/C_p$.
≠ Obtained from data inversion with (5).
§ *Isaak et al.* [1989].

Figure 12 with those obtained by our inversion procedure and the experimental results of *Isaak et al.* [1989]. All the values agree to within 2-4 % over the 300-2000 K range.

7. GRÜNEISEN PARAMETERS

Thermal and Microscopic Parameters

The properties studied in the previous sections are also involved in the calculation of the thermal Grüneisen parameter, γ, which is extensively used for calculating the adiabatic gradient of the mantle. Macroscopically, γ is defined by

$$\gamma = \alpha K_T V/C_V = V[\partial P/\partial U]_V \qquad (23)$$

and the values calculated with our anharmonic C_V and the α and K_T values obtained from our data inversion are given in Table 7. The results agree to within 10% with the figures reported by *Isaak et al.* [1989] or *White et al.* [1985] which are also included in Table 7.

Originally, this parameter was introduced by *Grüneisen* [1912] in a microscopic way in the form of a vibrational mode parameter γ_{iT}:

$$\gamma_{iT} = -(\partial \ln \nu_i/\partial \ln V)_T. \qquad (24)$$

We will note γ_m the Grüneisen parameter which can be expressed in terms of these microcopic parameters. For the special case of an harmonic solid, one has [Slater, 1939]

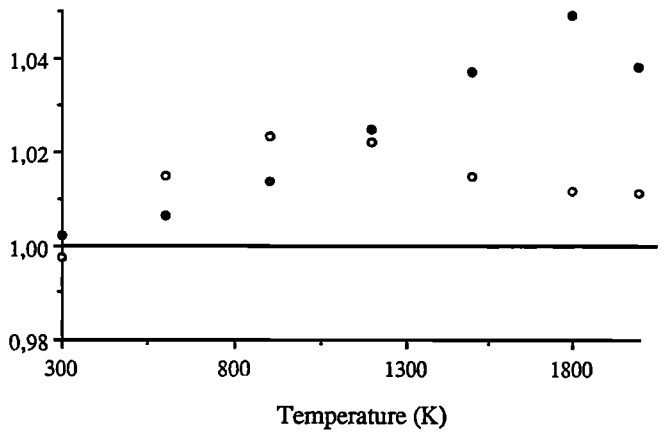

Fig. 12. Comparison of the K_T values of *Isaak et al.* [1989] with those obtained from data inversion with (5) (open circles) or from (22) (solid circles). Values taken from Table 6 are normalized to the values of K_T of *Isaak et al.* [1989].

TABLE 7. Grüneisen parameters of forsterite

	macroscopic		microscopic		
T, K	γ*	γ†	γ_m≠	γ_m §	γ_m#
300	1.29	1.28	1.19 [1.22]	1.21 [1.24]	1.36 [1.38]
600	1.17	1.10	1.06 [1.09]	1.10 [1.13]	1.29 [1.32]
900	1.15	1.07	0.99 [1.02]	1.03 [1.06]	1.23 [1.27]
1200	1.15	1.07	0.93 [0.97]	0.97 [1.01]	1.16 [1.21]
1500	1.15	1.07	0.87 [0.92]	0.91 [0.96]	1.09 [1.15]
1800	1.14	1.06	0.81 [0.87]	0.85 [0.91]	1.03 [1.10]
2000	1.14	1.06	0.76 [0.83]	0.79 [0.86]	0.99 [1.06]

* Data from *Isaak et al.* [1989], obtained from (23).
† Calculated from equation (23) with the present α, K_T, and C_V.
≠ Calculated with equation (29) and K_T=128 GPa; all the modes are used. The first value is obtained with all terms of the right-hand side of (29) , the values in brackets represent the first term of the right-hand side of (29).
§ Same as previous column but the γ_{iT} of the stretching modes of the SiO_4 tetrahedra are calculated with the Si-O bulk modulus of 190 GPa reported by *Kudoh and Takéuchi* [1985].
# Calculated with equation (29) with the lattice modes only (ν_i < 500 cm^{-1}).

$$\gamma_m = \Sigma \gamma_i C_{Vi}^h / \Sigma C_{Vi}^h \qquad (25)$$

where the harmonic calculation is emphasized by the superscript h.

The parameters calculated with (23) and (25) should be equal, but it has been found that eqn (25) gives values too small with respect to those obtained with (23) [e.g., *Chopelas*, 1990]. *Price et al.* [1987] suggested that part of the discrepancy arises from the intrinsic anharmonic contribution to γ_m. Hence, in this section we will first derive a general relationship between γ_m and the individual mode parameters in the case of an anharmonic solid. But application of this relationship to forsterite, for which a great many mode parameters can be determined [*Chopelas*, 1990; this work] still underestimates γ. We will finally discuss possible reasons for the discrepancy between the macroscopic and microscopic parameters and describe a sampling method which would allow to obtain consistency between the microscopic and macroscopic thermal parameters.

Anharmonic Grüneisen Parameters

The Helmholtz free energy of an harmonic crystal is

$$\begin{aligned} F &= F_0 - kT \Sigma \ln Z_i \\ &= F_0 + kT \Sigma \{(h\nu_i/2kT) + \ln[1 - \exp(h\nu_i/kT)]\} \\ &= F_0 + kT \Sigma U_i^h. \end{aligned} \qquad (26)$$

Differentiating with respect to volume, one has

$$P = -(\partial F/\partial V)_T = P_0 + (1/V) \Sigma \gamma_{iT} U_i^h, \qquad (27)$$

where P_0 is the pressure at 0 K. This expression is in fact the Mie-Grüneisen equation of state. Differentiating further and making use of (12), in introducing intrinsic anharmonicity one obtains

$$\begin{aligned} (\partial P/\partial T)_V = (1/V) \Sigma \{ &\gamma_{iT} [a_i U_i^h + C_{Vi}^h (1 - a_i T)] \\ &+ (\partial \gamma_{iT}/\partial T)_V U_i^h \} = \alpha K_T. \end{aligned} \qquad (28)$$

Finally, the microscopic Grüneisen parameter is thus given by:

$$\gamma_m = \Sigma\, \gamma_{iT}\, C_{vi}^{h}/C_v + \Sigma\, \gamma_{iT}\, a_i\, (U_i^{h} - T\, C_{vi}^{h})/C_v + \Sigma\, \gamma_{iT}\, (\partial \gamma_{iT}/\partial T)_V\, U_i^{h}/C_v. \quad (29)$$

This equation, which accounts for anharmonicity, represents so far the most general relation between the thermal and the microscopic Grüneisen parameters. In the limit of high temperatures, this equation reduces to

$$\gamma_m = \Sigma\, \gamma_{iT}/n + T\, \Sigma\, (\partial \gamma_{iT}/\partial T)_V, \quad (30)$$

and we thus conclude as usual that γ_m is the average of the mode Grüneisen parameters only if these are not functions of temperature at constant volume.

Application to Forsterite

In this section, we assess the importance of the various terms of (29) from the spectroscopic measurements on forsterite. Only the optic modes are taken into account. Because the data for all active modes are not known, we represent the 16 modes lying between 800 and 1000 cm^{-1} by the five well-determined Raman modes which are treated as Einstein oscillators. The remaining 65 modes are modeled by the other 13 observed Raman modes.

The major term of the right-hand side of equation (29) is the first one. The variation of $(\partial v_i/\partial P)_T$ with temperature is unknown because of the lack of spectroscopic measurements at simultaneously high pressure and temperature. Hence, we will first assume that this derivative is constant and evaluate (29) as a function of T from the actual values of K_T and v_i at different temperatures. With this assumption, this term decreases from 1.22 at 300 K to 0.97 at 1200 K and 0.83 at 2000 K (Table 7). The two other terms of the right-hand side of (29) are negative and contribute significantly less, being of the order of 10^{-1} and 10^{-2} between 300 and 2000 K, respectively (Table 7). Their effect is to lower the values calculated with only the first term of the right-hand side of (29) by 2-3% at 300 K and 10% at 2000 K. If the agreement between thermal Grüneisen parameters calculated with equations (23) and (29) is fair at 300 K, the parameter calculated with (23) reaches a high-temperature limit of about 1.15 [*Isaak et al.*, 1989] or 1.06 (this work) whereas that obtained from (29) decreases continuously with temperature down to 0.8 at 2000 K. The disagreement at high temperatures is thus real, even when considering the scatter in the reported macroscopic γ [*Boehler*, 1982; *Anderson and Suzuki*, 1983; *Isaak et al.*, 1989].

This difference can be attributed to several effects. First, too few modes would be taken into account in the calculation of γ_m with (29), i.e., the 18 Raman modes used would not represent correctly the optic modes of forsterite. This explanation appears unlikely, however, because similar results are obtained when the IR data of *Hofmeister et al.* [1989] for 15 additional modes are included in the calculations.

Another reason for the discrepancy could originate in the fact that forsterite has strong (Si-O) and weak (Mg-O) bonds [*Hazen and Finger*, 1982; *Kudoh and Takeuchi*, 1985]. The existence of contrasted bonds is partly reflected in the $(\partial \ln v_i/\partial P)_T$ values which are smaller for the Si-O stretches than for the lattice modes (Figure 7). The above observations suggest, as emphasized by *Sherman* [1980] in the case of molecular crystals, the separation of the crystal vibrations in two groups: a first one related to the internal vibrations of the SiO_4 tetrahedra and a second one related to lattice vibrations. The γ_{iT} of the lattice modes would then be calculated with the mean bulk modulus of the lattice (in this case the crystal bulk modulus or that of the Mg-O bond). We can then propose polyhedral Grüneisen parameters for the internal vibrations with the Si-O bond bulk modulus ($K_{TSi\text{-}O}$). The γ_{iT} for the internal modes would thus be written as

$$\gamma_{iT} = K_{TSi\text{-}O}\, (\partial \ln v_i/\partial P). \quad (31)$$

The Grüneisen parameter computed with (29) and (31) agrees better with that obtained from (23) at 300 K, but it still decreases with temperature to reach 0.86 at 2000 K (Table 7). Thus a significant improvement is obtained in this way, for the results (Table 7) agree to within 10% between 300 and 2000 K with γ as given by (23). But for the moment there are no clear theoretical explanations for this procedure. It could be justified by the existence of a sublattice which undergoes most of the structural changes and in which rigid, isolated SiO_4 units are embedded. In contrast, the classical approach for calculating γ_m from the γ_{iT} should work for minerals having only one kind of polyhedra, or different polyhedra with similar elastic properties, of which perovskite structures are the most important examples [*Williams et al.*, 1987; *Hemley et al.*, 1989].

We emphasize, however, that a different explanation could be proposed for the discrepancy between Grüneisen parameters calculated with (23) and (29). Little is in fact known about the variation of $(\partial v_i/\partial P)_T$ with temperature. The available data [*Dietrich and Arndt*, 1982] are sketchy and suggest that this derivative decreases with temperature, in which case the disagreement could be worse still. But moderate increases of this derivative are predicted if one assumes that vibrational frequencies are mainly determined by the volume [*Richet et al.*, 1991], and such increases could account for the observed discrepancy at high temperatures. Measurements of $(\partial v_i/\partial P)_T$ at different temperatures are thus badly needed to assess the influence of this derivative on the various terms of (29).

In summary, the example of forsterite shows that accurate experimental C_p data can be used to obtain reliable values of α and K_T at high temperatures from the room-temperature values of these parameters and an anharmonic calculation of C_v. Of course, this is not possible for mantle minerals when C_p is not known experimentally. If, as is usually the case, α is also unknown, then the importance of the anharmonic contributions to C_p makes it difficult to calculate C_p from spectroscopic data at high temperatures. In addition, the current discrepancies between Grüneisen parameters calculated from macroscopic and microscopic data also prevents reliable application of spectroscopic measurements to quantitative modeling of thermodynamic properties of mantle minerals. As pointed out above, this discrepancy requires spectroscopic measurements at both high temperature and high pressure in order to be resolved. In addition, efforts should be made to devise ways of determining the temperature dependence of thermal expansion coefficients from spectroscopic data.

Acknowledgments. We thank Fredo Vaucelle and Christophe Sotin for help in computer programing, B. Reynard for fruitful discussions, O.L. Anderson, A. Chopelas and G. Helffrich for helpful reviews. O. Jaoul and Y. Gueguen kindly provided the samples used in this study. Contribution CNRS-INSU-DBT 237.

REFERENCES

Anderson, O.L., and I. Suzuki, Anharmonicity of three minerals at high temperature: forsterite, fayalite, and periclase, *J. Geophys. Res., 88*, 3549-3556, 1983.

Anderson, O.L., and K. Zou, Thermodynamic functions and properties of MgO at high compression and high temperature, *J. Phys. Chem. Ref. Data, 19*, 69-83, 1990.

Ashida T., S. Kume, and E. Ito, Thermodynamic aspects of phase boundary among α-, β, and γ-Mg_2SiO_4, in *High-Pressure Research in Geophysics*, edited by M.H. Manghnani and Y. Syono, pp. 269-274, AGU, Washington, D.C, 1987.

Berman, R.G., and T.H. Brown, Heat capacity of minerals in the system Na_2O-K_2O-CaO-MgO-FeO-Fe_2O_3-Al_2O_3-SiO_2-TiO_2-H_2O-CO_2: Representation, estimation, and high-temperature extrapolation, *Contrib. Mineral. Petrol., 89*, 168-183, 1985.

Besson, J.M., Pinceaux, J.P., Anastopoulos, C., and Velde, B., Raman spectra of olivine up to 65 kilobars, *J. Geophys. Res., 87*, 10773-10775, 1982.

Boehler, R., Adiabats of quartz, coesite, olivine and magnesium oxide to 50 kbar and 1000 K, and the adiabatic gradient in the Earth mantle, *J. Geophys. Res., 87*, 5501-5506, 1982.

Chopelas, A., Thermochemical properties of forsterite at mantle pressures derived from vibrational spectroscopy, *Phys. Chem. Miner., 17*, 149-156, 1990.

Choudury, N., S.L. Chaplot, and K.R. Rao, Equation of state and melting point of forsterite, *Phys. Chem. Miner., 16*, 599-605, 1989.

Dietrich, P., and J. Arndt, Effects of pressure and temperature on the physical behaviour of mantle-relevant olivine, orthopyroxene and garnet II, Infrared absorption and Gruneisen-parameters, in *High Pressure Research in Geoscience*, edited by W. Schreyer, pp. 307-309, E. Schweizerbart'sche, Stuggart, Germany, 1982.

Fei, Y., and S.K. Saxena, An equation for the heat capacity of minerals, *Geochim. Cosmochim. Acta, 51*, 251-254, 1987*a*.

Fei, Y., and S.K. Saxena, A thermochemical data base for phase equilibria in the system Fe-Mg-Si-O at high pressure and temperature, *Phys. Chem. Miner., 13*, 311-324, 1987*b*.

Gillet, Ph., J.M. Malezieux, and M.C. Dhamelincourt, MicroRaman multichannel spectroscopy up to 2.5 GPa using a sapphire anvil cell: experimental set-up and some applications, *Bull. Minéral., 111*, 1-15, 1988.

Gillet, Ph., F. Guyot, and J.M. Malezieux, High pressure and high temperature Raman spectroscopy of Ca_2GeO_4: some insights on anharmonicity, *Phys. Earth Planet. Int., 58*, 141-154, 1989.

Gillet, Ph., A. Le Cléac'h, and M. Madon, High-temperature Raman spectroscopy of SiO_2 and GeO_2 polymorphs: anharmonicity and thermodynamic properties at high-temperatures, *J. Geophys. Res., 95*, 21635-21655, 1990.

Grüneisen, E., Theorie des festen zustandes einatomiger elemente, *Ann. Phys., 39*, 257-306, 1912.

Haas, J.L., Jr, and J.R. Fisher, Simultaneous evaluation and correlation of thermodynamic data, *Am. J. Sci., 276*, 525-545, 1976.

Hazen, R.M., and Finger, L.W., Comparative Crystal Chemistry, John Wiley and Sons, New York, 1982.

Hemley, R.J., R.E., Cohen, A. Yeganeh-Haeri, H.K. Mao, and D.J. Weidner, Raman spectroscopy and lattice dynamics of $MgSiO_3$ perovskite, in *Perovskite: A Structure of Great Interest to Geophysics and Materials Science, Geophys. Monogr. Ser., 45*, edited by A. Navrotsky and D.J. Weidner, pp. 35-44, AGU, Washington, D.C., 1989.

Hofmeister, A.M., Single-crystal absorption and reflection infrared of forsterite and fayalite, *Phys. Chem. Miner., 14*, 499-513, 1987.

Hofmeister, A.M., J. Xu, H.K. Mao, P.M. Bell, and T.C. Hoering, Thermodynamics of Fe-Mg, olivines at mantle pressure: mid- and far-infrared spectroscopy at high pressure, *Am. Mineral., 74*, 281-306, 1989.

Isaak, D.G., O.L. Anderson, and T. Goto, Elasticity of single-crystal forsterite measured to 1700 K, *J. Geophys. Res., 94*, 5895-5906, 1989.

Kajiyoshi , K., High-temperature equation of state for mantle minerals and their anharmonic properties, M.S. Thesis, Okayama University, Okayama, Japan, 1986. (Quoted by *Isaak et al.* [1989]).

Kelley, K.K., Specific heats at low temperatures of magnesium orthosilicate and magnesium metasilicate, *J. Am. Chem. Soc., 65*, 339-341, 1943.

Kieffer, S.W., Thermodynamics and lattice vibrations of minerals 3, Lattice dynamics and an approximation for minerals with application to simple substances and framework silicates, *Rev. Geophys., 17*, 827-849, 1979.

Kudoh, Y., and Y. Takéuchi, The crystal structure of forsterite Mg_2SiO_4 under pressure up to 149 kbar, *Z. Kristallogr., 171*, 291-302, 1985.

Mammone, J.F., and S.K. Sharma, Pressure and temperature dependence of the Raman spectra of rutile-structure oxides, *Year Book, Carnegie Inst. Washington, 78*, 369-373, 1979.

McMillan, P.F., and A.M. Hofmeister, Infrared and Raman spectroscopy, in *Spectroscopic Methods in Mineralogy and Geology, Reviews in Mineralogy*, vol. 18, edited by F.C. Hawthorne, pp. 99-159, Mineralogical Society of America, Whashington D.C., 1988.

Orr, R.L., High temperature heat contents of magnesium orthosilicate and ferrous orthosilicate, *J. Am. Chem. Soc., 75*, 528-529, 1953.

Price, G.D., S.C. Parker, and M. Leslie, The lattice dynamics and thermodynamics of the Mg_2SiO_4 polymorphs, *Phys. Chem. Miner.*, 15, 181-190, 1987.

Rao, K.R., S.L. Chaplot, N. Choudury, S. Ghose, J.M. Hastings and L.M. Corliss, Lattice dynamics and inelastic neutron scattering from forsterite, Mg_2SiO_4: phonon dispersion relation, density of states and specific heat, *Phys. Chem. Miner., 16*, 83-97, 1988.

Richet, P., and Y. Bottinga, Anorthite, andesine, diopside, wollastonite, cordierite and pyrope: thermodynamics of melting, glass transitions, and properties of the amorphous phases, *Earth Planet. Sci. Lett., 67*, 415-432, 1984.

Richet, P., and G. Fiquet, High-temperature heat capacity and premelting of minerals in the system CaO-MgO-Al_2O_3-SiO_2, *J. Geophys. Res., 96*, 445-456, 1991.

Richet, P., Y.Bottinga, L. Deniélou, J.P. Petitet, and C. Téqui, Thermodynamic properties of quartz, cristobalite and amorphous SiO_2: drop calorimetry measurements between 1000 and 1800 K and a review from 0 to 2000 K, *Geochim. Cosmochim. Acta, 46*, 2639-2658, 1982.

Richet, P., Ph. Gillet and G. Fiquet, Thermodynamic properties of minerals: macroscopic and microscopic approaches. *Adv. Phys. Geochem.*, in press, 1991.

Robie, R.A., B.S. Hemingway, and H. Takei, Heat capacities and entropies of Mg_2SiO_4, Mn_2SiO_4, and Co_2SiO_4 between 5 and 380 K, *Am. Mineral., 67*, 470-482, 1982.

Saxena, S.K., Assessment of thermal expansion, bulk modulus, and heat capacity of enstatite and forsterite. *J. Phys. Chem. Solids, 49*, 1233-1235, 1988.

Saxena, S.K., Assessment of bulk modulus, thermal expansion and heat capacity of minerals, *Geochim. Cosmochim. Acta, 53*, 785-789, 1989.

Sherman, W.F., Bond anharmonicities, Grüneisen parameters and pressure-induced shifts, *J. Phys. C Solid State. Phys., 13*, 4601-4613, 1980.

Slater, J.C., *Introduction to Chemical Physics*, 521 pp, McGraw Hill, New York, 1939.

Sotin, C., Contribution à l'étude de la structure et de la dynamique interne des planètes, Thèse, 395 pp., Université de Paris VII, 1986.

Suzuki, I., O.L. Anderson, and Y. Sumino, Elastic properties of a single-crystal forsterite Mg_2SiO_4, up to 1200 K, *Phys. Chem. Miner., , 10*, 38-46, 1983.

Tarantola, A., and B. Valette, Generalized non-linear inverse problems solved using the least square criterion, *Rev. Geophys., 20*, 219-232, 1982.

Watanabe, H., Thermochemical properties of synthetic high-pressure compounds relevant to the Earth's mantle, in *High-Pressure Research in Geophysics*, edited by S. Akimoto and M.H. Manghnani, pp. 441-464, D. Reidel, Hingham Mass., 1982.

White, G.K., R.B. Roberts, and J.G. Collins, Thermal properties and Grüneisen functions of forsterite, Mg_2SiO_4, *High Temp. High Pressures*, 17, 61-66, 1985.

Williams, Q., R. Jeanloz, and P.F. MacMillan, Vibrational spectrum of $MgSiO_3$ perovskite: zero pressure Raman and mid-infrared spectra to 27 GPa, *J. Geophys. Res., 92*, 8116-8128, 1987.

G. Fiquet and Ph. Gillet, Laboratoire de Minéralogie Physique, CAESS (UPR 4661), Université de Rennes I, 35042 Rennes Cedex, France.

F. Guyot and P. Richet, Département des Géomatériaux, Institut de Physique du Globe, 4 place Jussieu, 75005 Paris, France.

(Received November 5, 1990;
revised January 23, 1991;
accepted February 28, 1991.)